

Synthesis and Crystal Structure of $\text{Na}_4[(\text{TiO})_4(\text{SiO}_4)_3] \cdot 6\text{H}_2\text{O}$, a Rhombohedrally Distorted Sodium Titanium Silicate Pharmacosiderite Analogue

Mike S. Dadachov¹

Materials Division, Australian Nuclear Science and Technology Organisation, PMB 1, Menai, New South Wales 2234, Australia

and

William T. A. Harrison

Department of Chemistry, University of Western Australia, Nedlands, Western Australia 6907, Australia

Received April 15, 1997; in revised form August 25, 1997; accepted September 3, 1997

The synthesis and crystal structure of $\text{Na}_4[(\text{TiO})_4(\text{SiO}_4)_3] \cdot 6\text{H}_2\text{O}$, a new hydrated sodium titanium silicate with the rhombohedrally distorted pharmacosiderite structure type, are reported. $\text{Na}_4[(\text{TiO})_4(\text{SiO}_4)_3] \cdot 6\text{H}_2\text{O}$ was synthesized as a powder by the low temperature hydrothermal crystallization of an alkaline titanium silicate gel prepared via a novel peroxide route. Its structure was determined and refined by the Rietveld method using X-ray powder data. The three-dimensional framework of $\text{Na}_4[(\text{TiO})_4(\text{SiO}_4)_3] \cdot 6\text{H}_2\text{O}$ is built up from clusters of four edge-sharing TiO_6 octahedra, connected by tetrahedrally coordinated silicon atoms (isolated SiO_4 groups). The large extra-framework cages contain water molecules and are linked to each other via eight-membered rings ($\sim 5 \text{ \AA}$ in diameter). Two distinct Na cations are located: one in the off-center position of the eight-membered ring and another in the internal corner of cage. Crystal data: $\text{Na}_4[(\text{TiO})_4(\text{SiO}_4)_3] \cdot 6\text{H}_2\text{O}$, $M_r = 719.8$, rhombohedral, space group $R\bar{3}m$ (No. 160), $a = 7.8124(6) \text{ \AA}$, $\alpha = 88.794(9)^\circ$, $V = 476.50(6) \text{ \AA}^3$, $Z = 1$, $R_p = 0.09$, $R_{wp} = 0.12$.

© 1997 Academic Press

INTRODUCTION

Mixed-framework minerals and synthetic compounds with structures built up from octahedral and tetrahedral building units linked together through oxygen atom bridges are of great interest, particularly with respect to host-guest chemistry, structural diversity, ion-exchange and adsorption properties, and possible shape-selective catalytic activity (1–4).

The large class of titanium silicate minerals, built up from TiO_6 and SiO_4 building blocks, is represented by more than

70 examples (5). In the last 30 years, researchers have attempted to prepare synthetic titanium silicates by both high temperature solid state ceramic methods and hydrothermal crystallizations. The synthetic analogues of the minerals natisite $\text{Na}_2(\text{TiO})[\text{SiO}_4]$ (6) and its polymorphic modification $\text{Na}_8\text{Ti}_{3.5}\text{O}_2(\text{OH})_2[\text{SiO}_4]_4$ (7), zorite $\text{Na}_6[\text{Ti}(\text{Ti}_{0.9}\text{Nb}_{0.1})(\text{Si}_6\text{O}_{17})_2(\text{O},\text{OH})_5] \cdot 11\text{H}_2\text{O}$ (8, 9), sitinakite $\text{Na}_2(\text{H}_2\text{O})_2(\text{Ti}_{3.8}\text{Nb}_{0.2})(\text{OH})\text{O}_5(\text{SiO}_4)_2 \cdot \text{K}(\text{H}_2\text{O})_{1.7}$ (10), fresnoite $\text{Ba}_2(\text{TiO})[\text{Si}_2\text{O}_7]$ (11, 12), $\text{K}_2\text{TiSi}_3\text{O}_9$, a titanium-containing analogue of wadeite (12, 13), and nenakevichite $(\text{Na},\text{Ca})(\text{Nb},\text{Ti})\text{Si}_2\text{O}_7 \cdot 2\text{H}_2\text{O}$ (14) have been reported.

We have recently prepared some new alkali metal titanium silicates by hydrothermal method. The crystal structures of orthorhombic $\text{K}_2\text{TiSi}_3\text{O}_9 \cdot \text{H}_2\text{O}$ (15) and $\text{Na}_3(\text{Na},\text{H})\text{Ti}_2\text{O}_2[\text{Si}_2\text{O}_6]_2 \cdot 2\text{H}_2\text{O}$ (16) were solved from powder data by *ab initio* methods. A large single crystal of monoclinic $\text{K}_4\text{Ti}_2\text{Si}_6\text{O}_{18} \cdot 2\text{H}_2\text{O}$ was grown and its structure was determined from single crystal data (17). The new titanosilicate open framework denoted ETS-10 (18), and the catalytically active layered phase $\text{Na}_4\text{Ti}_2\text{Si}_8\text{O}_{22} \cdot 4\text{H}_2\text{O}$ (19) have also been described.

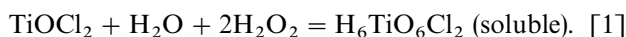
Recently, the phases $M_{4-x}\text{H}_x\text{Ti}_4\text{O}_4(\text{SiO}_4)_3 \cdot n\text{H}_2\text{O}$ ($M =$ alkali metal, $n = 4-8$) have been prepared as powders (20). These titanosilicates phases are isostructural with the open-framework hydrated iron arsenate mineral pharmacosiderite, $\text{KFe}_4(\text{OH})_4(\text{AsO}_4)_3 \cdot 6\text{H}_2\text{O}$ (21) and its analogues (22–24). Single crystals of $\text{Cs}_3\text{HTi}_4\text{O}_4(\text{SiO}_4)_3 \cdot 4\text{H}_2\text{O}$ [cubic, space group $P\bar{4}3m$, $a = 7.8301(9) \text{ \AA}$] may be prepared hydrothermally at elevated temperatures and pressures (25). In this paper we report the novel low-temperature synthesis and structure determination of $\text{Na}_4[(\text{TiO})_4(\text{SiO}_4)_3] \cdot 6\text{H}_2\text{O}$, a new rhombohedrally distorted titanosilicate pharmacosiderite.

¹To whom correspondence should be addressed.

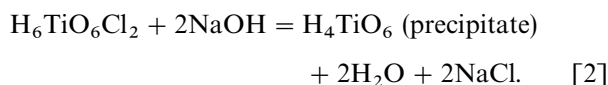
EXPERIMENTAL

Preparation. A major problem in mild hydrothermal synthesis of titanium silicates is finding a feasible source of titanium. Almost all known titanium compounds have very low solubility in water and other common solvents including strong acids and bases, thus making it difficult to prepare homogeneous titanium silicate gels analogous to the aluminosilicate gels used for zeolite crystallization. Crystallization of a non-homogeneous initial mixture of titanium- and silicon-containing precursors often results in formation of undesirable amorphous or semicrystalline phases as anatase, rutile, or layered alkaline metal titanates. Simple titanium alkoxides tend to hydrolyze rapidly, leading to poor gel homogeneity. Below, we describe two methods for preparing the water-soluble, "user-friendly" compound sodium peroxotitanate as a precursor in the preparation of homogenous (interacted Ti and Si) amorphous titanium silicate which can subsequently be crystallized.

Method 1. Hydrogen Peroxide was added to a stirred titanyl chloride TiOCl_2 solution (prepared from TiCl_4 via hydrolysis in 15% HCl in water solution with composition $\text{TiOCl}_2:\text{HCl}:\text{H}_2\text{O} = 15:15:70$ wt%):



Two mole equivalents of sodium hydroxide pellets were added to the resulting peroxy-titanyl chloride solution:

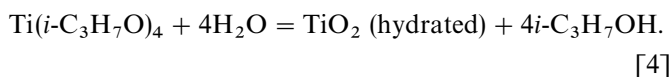


The solid peroxy-titanyl acid was filtered under suction and washed and dried in air, followed by reaction with sodium hydroxide to form the water soluble sodium peroxotitanate:



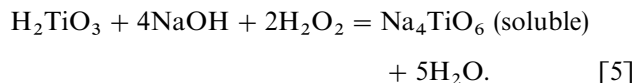
Silicasol Ludox HS-40 was used as a source of Si. It was added under stirring to the solution of Na_4TiO_6 (Si/Ti = 2) and the resulting mixture was destabilized and deperoxidized by aging (25–60°C).

Method 2. Hydrous titanium oxide $\text{TiO}_2 \cdot n\text{H}_2\text{O}$ was obtained from titanium isopropoxide by its hydrolysis in water:



Drying of the hydrous titanium oxide at 80°C resulted in the formation of the nearly stoichiometric compound H_2TiO_3 .

Hydrogen peroxide and sodium hydroxide in water were added to H_2TiO_3 to form water soluble sodium peroxotitanate:



Silicasol Ludox HS-40 (Si:Ti = 2) as a source of Si was added to the obtained solution. The resultant transparent solution again was deperoxidized by aging (25–60°C) to give amorphous sodium titanium silicate.

Crystallization of amorphous sodium titanium silicate. To 9 g of fine powder of dried (at 80°C) amorphous sodium titanium silicate, 30 ml of 1 M NaOH was added. Crystallization proceeded in a Teflon-lined autoclave ($V = 45$ ml) at 160°C for 100 h. The resulting crystalline material was washed with water and ethanol and dried at room temperature.

X-ray data collection, structure determination, and refinement.

The powder pattern for the initial phase identification and all subsequent diffraction data were obtained on a laboratory Siemens D500 powder diffractometer. An initial scan showed that sample was a very fine crystalline powder with a pattern resembling that of the cubic titanium silicate pharmacosiderite structure (20), but many diffraction peaks were split (Fig. 1). At this stage of analysis it

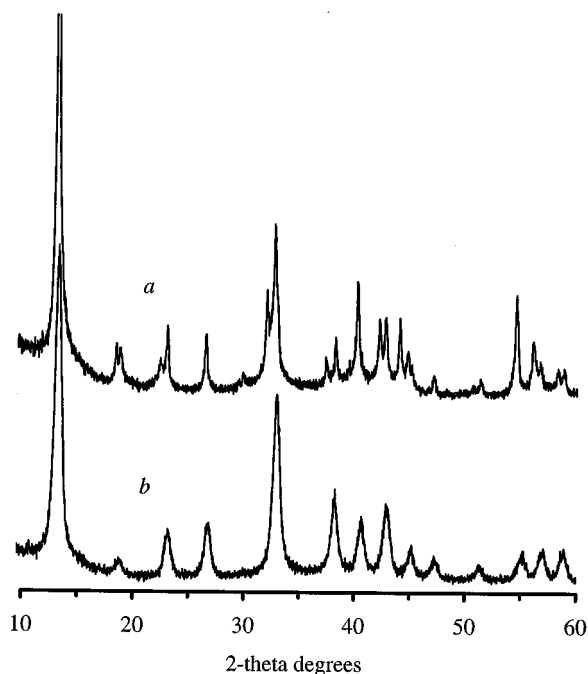


FIG. 1. Diffraction pattern of rhombohedrally distorted $\text{Na}_4[(\text{TiO})_4(\text{SiO}_4)_3] \cdot 6\text{H}_2\text{O}$ (a) and cubic $\text{K}_3\text{H}[(\text{TiO})_4(\text{SiO}_4)_3] \cdot 4\text{H}_2\text{O}$ analogue of titanium silicate pharmacosiderites (b) ($\text{CoK}\alpha$ radiation).

was assumed that the compound had a distorted phar-macosiderite type structure, which meant that more detailed diffraction data were needed for structure determination. Powder diffraction pattern was scanned in steps of 0.02° (2 Θ) over the angular range 10°–100° (2 Θ) and fixed-time counting (10 s) was employed. Indexed powder data for Na₄[(TiO)₄(SiO₄)₃]·6H₂O (rhombohedral unit cell with $a = 7.8123 \text{ \AA}$, $\alpha = 88.794^\circ$, and $V = 476.5 \text{ \AA}^3$) are presented in Table 1. The structural model was optimized by the Rietveld methods using the GSAS package (26) and started with the set of framework atomic coordinates given for rhombohedral Na₃H_x(H₂PO₄)_x[Ge₄O₄(GeO₄)₃]·4H₂O (27) (Ti replacing octahedral Ge; Si replacing tetrahedral

TABLE 1
X-ray Powder Diffraction Data for Na₄[(TiO)₄(SiO₄)₃]·6H₂O

<i>h</i>	<i>k</i>	<i>l</i>	2 Θ_{obs} (°)	d_{obs} (Å)	d_{calc} (Å)	I_{obs}
1	0	0	13.167	7.807	7.809	100
1	1	0	18.470	5.577	5.579	10
1	-1	0	18.829	5.472	5.465	9
1	1	1	22.445	4.599	4.604	8
1	-1	0	23.073	4.475	4.477	13
2	0	0	26.555	3.897	3.904	11
2	-1	0	29.952	3.463	3.463	5
2	1	1	32.050	3.242	3.244	18
2	-1	1	32.762	3.173	3.177	29
2	-1	-1	32.980	3.153	3.155	17
2	2	0	37.402	2.789	2.789	8
2	-2	0	38.298	2.728	2.732	11
2	2	1	39.520	2.648	2.652	7
3	0	0, 2 2 -1	40.268	2.600	2.603	20
3	1	0	42.273	2.482	2.484	14
3	-1	0	42.819	2.452	2.454	14
3	1	1	44.096	2.384	2.386	14
3	-1	-1	45.160	2.331	2.332	7
2	-2	2	47.196	2.236	2.238	5
3	2	0	48.270	2.189	2.186	5
3	2	-1	50.752	2.088	2.090	4
3	-2	-1	51.407	2.063	2.071	5
4	0	0	54.608	1.951	1.952	18
3	2	2	55.540	1.921	1.931	4
4	1	0	56.131	1.902	1.903	10
4	-1	0, 3 -2 2	56.750	1.883	1.884	7
4	-1	1	58.339	1.836	1.838	6
4	-1	-1	58.780	1.824	1.826	5
3	-3	0	58.852	1.821	1.821	6
3	-3	1	60.681	1.772	1.774	4
4	2	0	61.204	1.758	1.760	4
4	-2	0	62.307	1.730	1.731	6
4	3	0	69.194	1.576	1.577	7
4	-3	0	70.773	1.545	1.546	7
4	4	0	79.841	1.394	1.394	4
5	2	2	80.900	1.379	1.380	6
4	4	-1	81.931	1.365	1.366	5
4	4	2	84.850	1.326	1.326	4
5	-3	1	86.288	1.309	1.310	4
6	2	1	93.212	1.231	1.232	3

TABLE 2
Crystallographic Parameters for Na₄[(TiO)₄(SiO₄)₃]·6H₂O

Diffraction	Siemens D500
Radiation	CoK α , filtered
2 Θ range [°]	10–100
Step Scan increment [°]	0.02
Count time [s/step]	10
Peak shape	Pseudo Voigt
Background	Chebyshev polynomial
Crystal chemical formula	Na ₄ [(TiO) ₄ (SiO ₄) ₃]·6H ₂ O
Space group	<i>R3m</i> (No. 160)
<i>a</i> [Å]	7.8123 (6)
α [°]	88.794 (9)
<i>V</i> [Å ³]	476.50 (6)
Number of observations	4751
Number of reflections	148
Number of refined structural parameters	40
Number of Profile parameters	10
R_p [%]	9.59
R_{wp} [%]	12.31
R_F [%]	9.21
R_B [%]	7.6

Ge) in the acentric space group *R3m*, with fixed isotropic displacement factors of 0.01 Å² for all atoms.

The usual profile parameters and framework atomic positional parameters were refined to convergence. A subsequent difference Fourier synthesis showed the positions of nonframework cations and oxygen atoms of water molecules, which were distinguished from each other in the difference maps by relative peak heights and geometrical considerations. As a result of this analysis, two sodium cations and two oxygen atoms of water molecules were localized. Further refinement led to convergence, resulting in final stoichiometry of Na₄[(TiO)₄(SiO₄)₃]·6H₂O. The final crystallographic and Rietveld parameters for rhombohedrally-distorted sodium titanium silicate are listed in Table 2.

RESULTS

The Rietveld analysis confirms that Na₄[(TiO)₄(SiO₄)₃]·6H₂O is a rhombohedrally distorted phar-macosiderite type phase. The final fit between calculated and observed patterns is presented in Fig. 2. Final atomic positional parameters are given in Table 3, with selected bond distances and angles listed in Table 4.

Na₄[(TiO)₄(SiO₄)₃]·6H₂O contains 12 crystallographically distinct nonhydrogen atoms. There are two Ti centers, both of which are octahedrally coordinated by O atom neighbors. The octahedral connectivity via edges leads to Ti₄O₁₆ clusters at the unit-cell corners, with the four Ti and four central O atoms forming a “cubane”-like cluster (Fig. 3a). These Ti₄O₁₆ clusters are linked into a three-

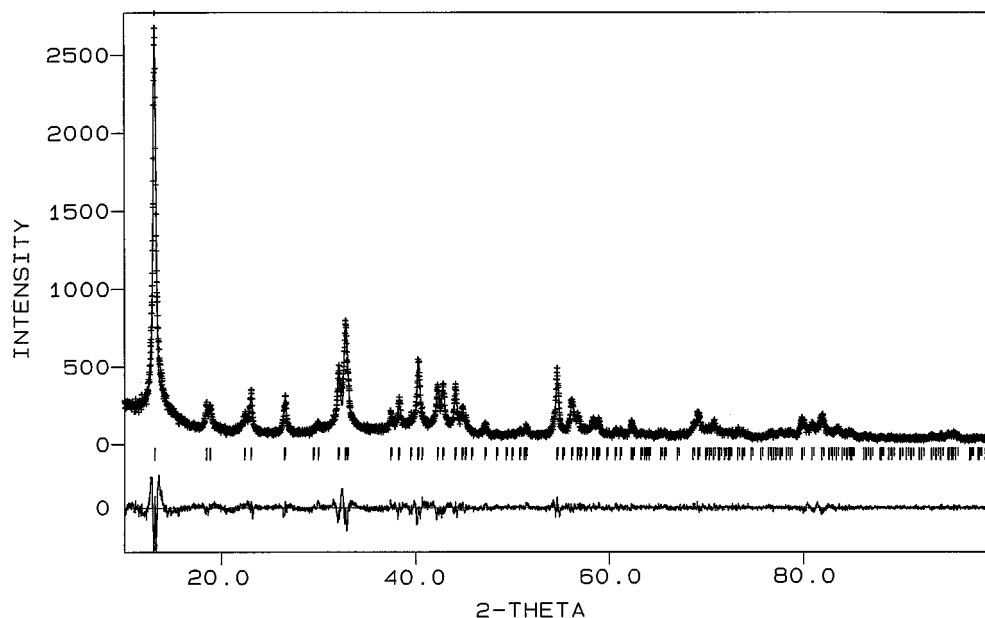


FIG. 2. Observed (crosses) and calculated (line) profiles (X-ray intensity vs 2θ) for the Rietveld refinement of $\text{Na}_4[(\text{TiO})_4(\text{SiO}_4)_3] \cdot 6\text{H}_2\text{O}$. The bottom curve is the difference plot on the same intensity scale.

dimensional framework by the single distinct Si atom (as a tetrahedral SiO_4 group, Fig. 3b) by way of Ti–O–Si–O–Ti bridges. In other words, Ti_4O_{16} can be described as four TiO_6 octahedra each sharing three edges with three other TiO_6 octahedra. Thus, the structural formula of the three-dimensional framework can be represented by either $[(\text{TiO})_4(\text{SiO}_4)_3]^{4-}$ or $[\text{Ti}_4\text{O}_4(\text{SiO}_4)_3]^{4-}$. This framework topology requires five crystallographically distinct O atoms in its rhombohedral modification: two of these, O(1) and O(2) are coordinated by three Ti atom neighbours in roughly pyramidal coordination, while O(3), O(4), and O(5) form Ti–O–Si bridges. The Ti/Si/O framework encloses spheroidal cavities, interconnected by a three-dimensional

channel network propagating along [100], [010], and [001]. The intercavity windows are eight-membered rings, built up from four SiO_4 and four TiO_6 units.

TABLE 4
Selected Bond Lengths (Å) and Angles ($^\circ$) for
 $\text{Na}_4[(\text{TiO})_4(\text{SiO}_4)_3] \cdot 6\text{H}_2\text{O}$

TABLE 3
Atomic Coordinates/Thermal Parameters for
 $\text{Na}_4[(\text{TiO})_4(\text{SiO}_4)_3] \cdot 6\text{H}_2\text{O}$

Atom	Site	x/a	y/a	z/a	U_{iso} (Å^2)
Ti(1)	3m	0.1300(20)	0.1300(20)	0.1300(20)	0.9
Ti(2)	m	-0.1436(13)	-0.1436(13)	0.1329(13)	0.9
Si	m	0.4891(29)	-0.0041(14)	-0.0041(14)	0.7
O(1)	3m	0.871(5)	0.871(5)	0.871(5)	1.0
O(2)	m	0.121(4)	0.121(4)	0.861(6)	1.0
O(3)	m	0.115(4)	0.115(5)	0.3636(34)	1.0
O(4)	m	-0.1342(34)	-0.1342(34)	0.401(4)	1.0
O(5)	1	-0.1299(24)	0.1163(30)	-0.3965(24)	1.0
Na(1)	3m	0.653(4)	0.653(4)	0.653(4)	2.5
Na(2)	m	0.910(4)	0.444(4)	0.444(4)	2.0
O(w1)	m	0.605(5)	0.296(4)	0.296(4)	2.0
O(w2)	m	0.546(5)	0.546(5)	0.215(5)	2.0

Ti(1)–O(2)	2.11(5)($\times 3$)	O(2)–Ti(1)–O(2)	84.8(21)
Ti(1)–O(3)	1.827(30)($\times 3$)	O(2)–Ti(1)–O(3)	172.0(22)
		O(2)–Ti(1)–O(3)	89.2(14)
		O(3)–Ti(1)–O(3)	96.1(21)
Ti(2)–O(1)	2.05(4)	O(1)–Ti(2)–O(2)	85.3(16)
Ti(2)–O(2)	2.068(33)($\times 2$)	O(1)–Ti(2)–O(4)	172.6(20)
Ti(2)–O(4)	2.097(3)	O(1)–Ti(2)–O(5)	88.2(12)
Ti(2)–O(5)	1.984(20)($\times 2$)	O(2)–Ti(2)–O(2)	87.0(24)
		O(2)–Ti(2)–O(4)	89.3(14)
		O(2)–Ti(2)–O(5)	88.9(15)
		O(2)–Ti(2)–O(5)	172.6(10)
		O(2)–Ti(2)–O(4)	89.3(14)
		O(4)–Ti(2)–O(5)	96.8(8)
		O(5)–Ti(2)–O(5)	94.5(12)
Ti(2)–Ti(1)	3.054(16)	Ti(1)–O(2)–Ti(2)	93.9(12)
Ti(2)–Ti(1)	3.022(15)		
Si(1)–O(3)	1.63(4)	O(3)–Si(1)–O(4)	117.8(27)
Si(1)–O(4)	1.628(13)	O(3)–Si(1)–O(5)	109.6(7)
Si(1)–O(5)	1.615(9)($\times 2$)	O(4)–Si(1)–O(5)	103.5(11)
Na(1)–O(1)	3.01(10)		
Na(1)–O(1)	3.04(4)($\times 3$)		
Na(2)–O(3)	3.07(4)($\times 2$)		
Na(2)–O(5)	2.843(22)($\times 2$)		
Na(2)–O(w1)	2.94(5)		
Na(2)–O(w2)	2.67(4)		

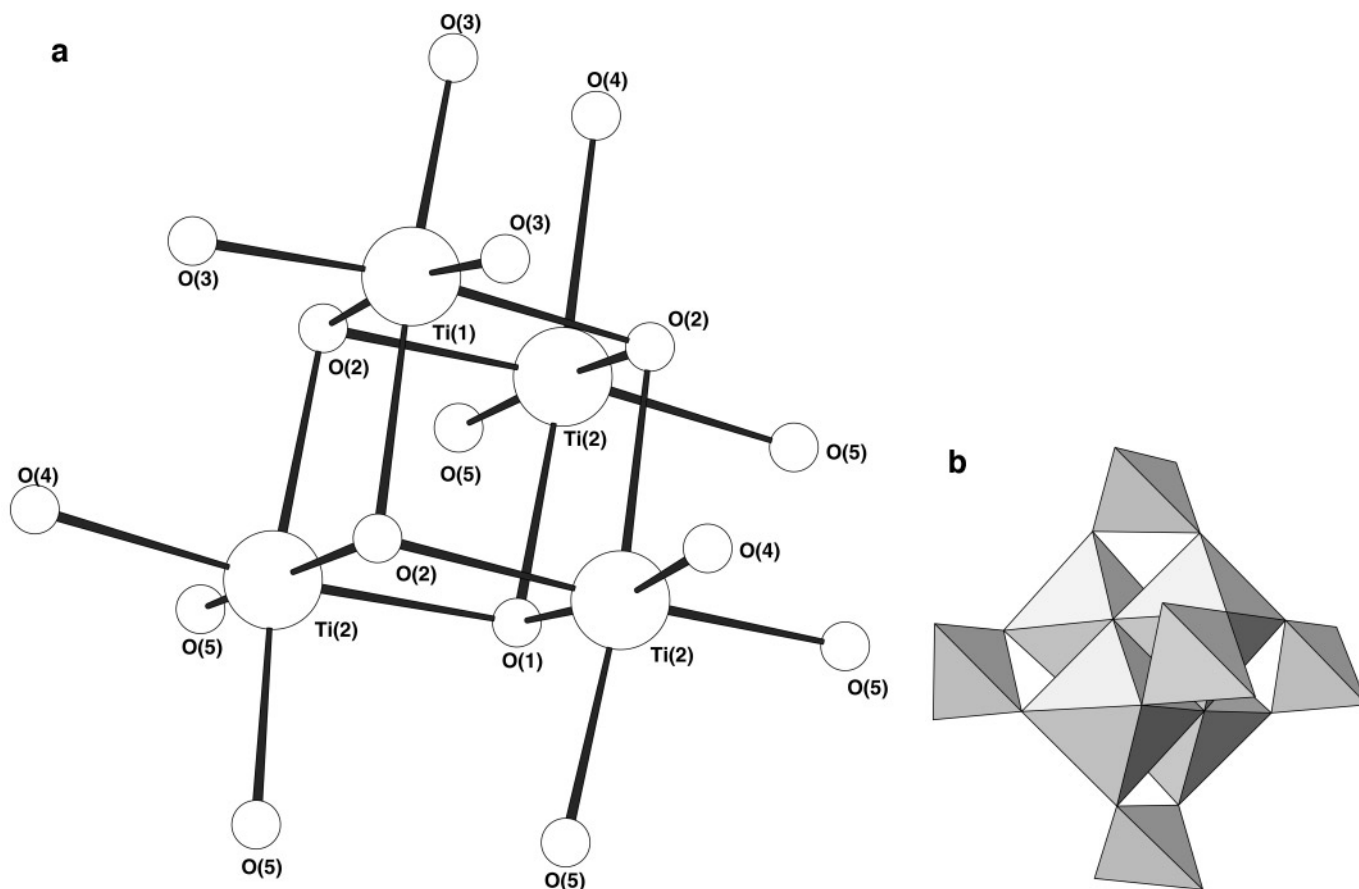


FIG. 3. Detailed $\text{Na}_4[(\text{TiO})_4(\text{SiO}_4)_3] \cdot 6\text{H}_2\text{O}$ structure showing a Ti_4O_{16} cluster (a) and its connectivity with SiO_4 tetrahedra (b).

As modelled here, the extraframework species in $\text{Na}_4[(\text{TiO})_4(\text{SiO}_4)_3] \cdot 6\text{H}_2\text{O}$ consist of an ordered distribution of two sodium cations and two water molecules. The most interesting feature of this structure is extraframework cations and their positioning in relation to the framework oxygens and water molecules (Fig. 4). Na(2) cations are located in off-center positions of eight membered rings and coordinated by six oxygens: four framework oxygens and two water oxygens. Thus, Na(2) coordination polyhedra may be presented as $[\text{Na}(2)\text{O}(3)_2\text{O}(5)_2\text{O}(w)_2]$. Oxygens of water molecules belong to neighboring cages and are located at opposite corners of Na polyhedra, i.e. in *trans* position. The coordination polyhedra of Na(2) are not connected with each other. Five oxygen–sodium distances are close to $\sim 3 \text{ \AA}$, but Na–O(w2) bond is noticeably oversaturated (2.67 \AA). However, sodium–oxygen polyhedra cannot be called octahedra, since the octahedral angles O–Na–O are highly distorted. Apparently, Na(2) positioned off center in the eight-membered rings contributes to the stabilization of the structure in the same way as well-centered large K and Cs cations in cubic pharmacosiderite

(25). Na(1) with $3m$ symmetry is positioned inside the cage. Such insertion of a cation into the cage has not been observed in the pharmacosiderite structure in its many compositional forms (arsenates (21,22), silicates (20,25), germanates (23,24), phosphates (2,31)). Na(1) is coordinated by four oxygens. Interestingly, though all Na(1)–O distances are almost the same ($3.01\text{--}3.04 \text{ \AA}$), the NaO_4 polyhedron must be described as a trigonal pyramid (not a tetrahedron) since Na(1) is located close to the plane of three O(4) oxygens. Thus, the O(1)–O(4) distances are about 0.7 \AA shorter than the O(4)–O(4) edge.

DISCUSSION

We have prepared and characterized $\text{Na}_4[(\text{TiO})_4(\text{SiO}_4)_3] \cdot 6\text{H}_2\text{O}$, a pharmacosiderite-type open-framework titanosilicate, by a novel synthetic method. Previously studied pharmacosiderite-type titanosilicates (20,25) were seen to crystallize in cubic symmetry in the space group $P\bar{4}3m$. The rhombohedral $R3m$ modification of the cubic pharmacosiderite structure has been observed previously for

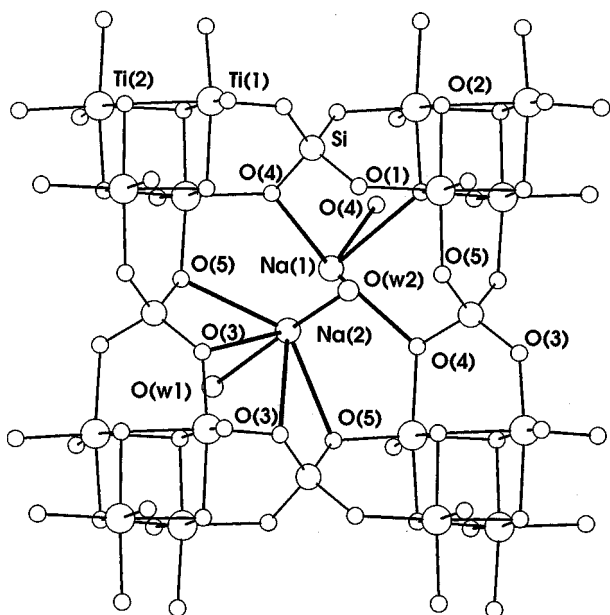


FIG. 4. A view of the crystal structure of $\text{Na}_4[(\text{TiO})_4(\text{SiO}_4)_3] \cdot 6\text{H}_2\text{O}$, showing the framework oxygens and water molecule environment of both sodium cations.

various compounds based on an all-germanium $[(\text{Ge}_4\text{O}_4)(\text{GeO}_4)_3]$ framework (27, 29), suggesting that this structural topology is relatively flexible, regardless of its atomic composition. Since SiO_4 tetrahedra are regarded as being essentially rigid, it was assumed that the flexibility of this structure arises from its octahedral component (29). In the structure of $\text{Cs}_3\text{H}[(\text{TiO})_4(\text{SiO}_4)_3] \cdot 4\text{H}_2\text{O}$ (20, 25), the large cesium cation occupies a position at the center of the 8-ring window, although Cs interactions with the oxygen atom of a water molecule also appear to be significant in determining the location of this atom. There are many other compositionally different cubic compounds with a pharmacosiderite framework, described by space group $P\bar{4}3m$, such as arsenate minerals (21, 22), Cs and K titanium silicates (20, 25) and Cs molybdenum phosphates prepared by both mild hydrothermal and high temperature solid state syntheses (2, 31). The large cations (K, Cs) are located in a special position $(\frac{1}{2}, \frac{1}{2}, 0)$ in all of the above structures. These cations are symmetrically bonded to eight oxygens, involving oxygens of four tetrahedral cations TO_4 , $T = \text{Si}, \text{P}, \text{Ge}$ at approximately 3.2 Å.

The sodium cation is too small to occupy the center of the intercavity 8-ring window. Here we postulate that the symmetry reduction from cubic to trigonal for $\text{Na}_4[(\text{TiO})_4(\text{SiO}_4)_3] \cdot 6\text{H}_2\text{O}$ occurs as a result of inclusion of the additional guest Na(1) cation and its interaction with the framework O(4) and O(1) atoms. As it was found in the structure of this compound the additional sodium Na(1) primarily interacts with framework oxygens O(4) and O(1). The result of this interaction, cation-oxygen distances are

much shorter (about ~ 0.2 Å) than observed in cubic structure. By varying the Ti–O–Ti bond angles, the Ti_4O_{16} cluster undergo a squashing or stretching transformation along the (cubic) $\langle 111 \rangle$ direction, resulting in symmetry reduction. We note that the transformation from $P\bar{4}3m$ to $R3m$ is a well-behaved, and presumably second-order, symmetry-reducing phase transition (30). We note that the different cation arrangement leads to different water content (four H_2O per unit cell for Cs, Six H_2O per unit cell for Na), assuming that the simple, fully ordered Na/ H_2O model described above is adequate. In rhombohedral/cubic $\text{Na}_3\text{H}_x(\text{H}_2\text{PO}_4)_x[(\text{GeO})_4(\text{GeO}_4)_3] \cdot 4\text{H}_2\text{O}$ (27) the situation may be more complex, since the extra framework anion type also appeared to be significant in determining the crystal symmetry for this material.

Further titanosilicates and related phases are now being characterized and will be described later.

ACKNOWLEDGMENT

We thank the Australian Research Council for partial financial support.

REFERENCES

1. R. Szostak, "Molecular Sieves, Principles of Synthesis and Identification." Van Nostrand, New York, 1989.
2. L. A. Mundi, K. G. Strohmaier, and R. C. Haushalter, *Inorg. Chem.* **30**, 154 (1991).
3. T. Loiseau and G. Férey, *J. Chem. Soc. Chem. Commun.*, 1197 (1992).
4. R. G. Anthony, C. V. Philip, and R. G. Dosch, *Waste Manage.* **13**, 503 (1993).
5. Yu. A. Pyatenko, A. A. Voronkov and Z. V. Pudovkina, "The Mineralogical Crystal Chemistry of Titanium," p. 155. Nauka, Moscow, 1976.
6. A. V. Nikitin, V. Vilyukhin, B. N. Litvin, O. K. Melnikov, and N. V. Belov, *Sov. Phys. Dokl.* **9**, 625 (1965).
7. E. B. Sokolova, A. N. Yamnova, Yu. K. Egorov-Tismenko, and A. P. Chomyakov, *Sov. Phys. Dokl.* **9**, 1136 (1965).
8. A. N. Mer'kov, I. V. Bussen, E. A. Goiko, E. A. Kul'chitskaya, Y. P. Men'shikov, and A. P. Nedorezova, *Zap. Vses. Mineralog. O-va* **102**, 54 (1973).
9. P. A. Sandomirskii and N. V. Belov. *Kristallografiya* **24**, 1198 (1978).
10. E. B. Sokolova, R. K. Rastsvetaeva, V. I. Andrianov, Yu. K. Egorov-Tismenko, and Yu. P. Men'shikov. *Sov. Phys. Dokl.* **34**, 114 (1989).
11. P. B. Moore and S. J. Louisnathan, *Z. Kristallogr.* **130**, 438 (1969).
12. S. A. Markgraf, A. Halliyal, A. S. Bhalla, and R. E. Newnham, *Ferroelectrics* **62**, 17 (1985).
13. N. G. Shumyatskaya, V. A. Blinov, A. A. Voronkov, V. V. Ilyukhin, and N. V. Belov, *Sov. Phys. Dokl.* **18**, 17 (1973).
14. J. Rocha, P. Brandao, Z. Lin, A. Kharlamov, and M. W. Anderson, *Chem. Commun.*, 669 (1996).
15. M. S. Dadachov and A. LeBail, *Eur. J. Solid State Inorg. Chem.* **34**, 381 (1997).
16. M. S. Dadachov, J. Rocha, A. Ferreira, Z. Lin, and M. W. Anderson, *Chem. Commun.*, in press.
17. M. S. Dadachov and D. Graig, submitted for publication.
18. M. W. Anderson, O. Terasaki, T. Ohsuna, P. J. O'Malley, A. Philippou, S. P. Mackay, A. Ferreira, J. Rocha, and S. Lidin, *Phil. Mag. B* **71**, 813 (1995).

19. M. A. Roberts, G. Sankar, J. M. Thomas, R. H. Jones, H. Du, J. Chen, W. Pang, and R. Xu, *Nature* **381**, 401 (1996).
20. D. M. Chapman and A. L. Roe, *Zeolites* **10**, 730 (1990).
21. A. Zemann, *Tscherm. Miner. Petr. Mitt.* **3**, 1 (1948).
22. H. Nowotny and A. Wittmann, *Montash. Chem.* **85**, 558 (1954).
23. M. J. Buerger, W. A. Dollase, and I. Garaycochea-Wittke, *Z. Kristallogr.* **125**, 92 (1967).
24. G. I. Sturua, E. L. Belokoneva, M. A. Simonov, and N. V. Belov, *Dokl. Akad. Nauk SSSR* **242**, 1078 (1978).
25. W. T. A. Harrison, T. E. Gier, and G. D. Stucky, *Zeolites* **15**, 408 (1995).
26. A. C. Larson and R. B. Von Dreele, "GSAS User Guide." Los Alamos National Laboratory, New Mexico.
27. T. M. Nenoff, W. T. A. Harrison, and G. D. Stucky, *Chem. Mater.* **6**, 525 (1994).
28. D. H. Olson, *J. Phys. Chem.* **74**, 2758 (1970).
29. M. A. Roberts, A. N. Fitch, and A. V. Chadwick, *J. Phys. Chem Solids* **56**, 1353 (1995).
30. "International Tables for X-Ray Crystallography," Vol. A, p. 647. Kynoch Press, Birmingham, 1974.
31. R. C. Haushalter, *J. Chem. Soc. Chem. Commun.*, 1566 (1987).